Light-Driven, Reversible Spatiotemporal Control of Dynamic Covalent Polymers

David Reisinger, Alexander Sietmann†, Ankita Das†, Sarah Plutzar, Elisabeth Rossegger, Matthias Walluch, Stefan Holler-Stangl, Thomas S. Hofer, Fabian Dielmann, Frank Glorius*, and Sandra Schlögl**

†These authors contributed equally to this work.

D. Reisinger, S. Plutzar, E. Rossegger, S. Schlögl
Polymer Competence Center Leoben GmbH, Sauraugasse 1, 8700 Leoben, Austria
E-mail: sandra.schloegl@pccl.at

A. Sietmann, T. S. Hofer, F. Dielmann
Department of General, Inorganic and Theoretical Chemistry, University of Innsbruck, Innrain 80-82, 6020 Innsbruck, Austria
E-mail: fabian.dielmann@uibk.ac.at

A. Das, F. Glorius
Organisch-Chemisches Institut, University of Münster, Corrensstraße 40, 48149 Münster, Germany
E-mail: glorius@uni-muenster.de

M. Walluch, S. Holler-Stangl
Anton Paar GmbH, Anton-Paar Straße 20, 8054 Graz, Austria

Keywords: dynamic covalent polymers, reversible photoactivation, photoswitchable base catalysts, photopolymerization, multi-step reshaping, multi-step micro-imprinting

Dynamic covalent polymer networks exhibit a cross-linked structure like conventional thermosets and elastomers, although their topology can be reorganized by thermoactivated bond exchange. This characteristic enables a unique combination of repairability, recyclability and dimensional stability, crucial for a sustainable industrial economy. We herein report the application of a photoswitchable nitrogen superbase for the spatially resolved and reversible control over dynamic bond exchange within a thiol-ene photopolymer. By the exposure to UV or visible light, we successfully gain control over the associative exchange between thioester links and thiol groups, and thereby the macroscopic mechanical material properties, in a locally controlled manner. Consequently, the resulting reorganization of the global network topology enables us to utilize our material for previously unrealizable advanced applications such as spatially resolved, reversible reshaping as well as micro-imprinting over multiple steps. Finally, the presented concept contributes fundamentally to the evolution of dynamic polymers and provides universal applicability in covalent adaptable networks relying on a base-catalyzed exchange mechanism.

1. Introduction

Thermosetting and elastomeric polymers exhibit a three-dimensional covalently cross-linked network topology, which leads to dimensional stability, resistance to creep, and chemical exposure even at high operating temperatures. Finally, their high strength to weight ratios make them ideal candidates for high performance applications such as construction and machine parts, adhesives, protective coatings, sealings as well as matrix materials in numerous types of composites.[1,2,3] Thermoplastic materials, on the other hand, consist of individual (chemically) non-crosslinked polymer chains. They merely interact via physical intermolecular forces, which rapidly weaken at elevated temperatures. The increased chain mobility results in a soft viscous state, enabling reshaping, welding, and recycling through, e.g., extrusion, injection and compression molding, or calendaring.[2,3,4]

So-called covalent adaptable networks (CANs) are designed to combine the advantageous aspects of thermosetting and thermoplastic materials. In response to an external stimulus (most often heat), their three-dimensional covalently cross-linked network structure can be reorganized by a dynamic exchange of covalent bonds. Owing to an associative reaction pathway, the global number of cross-links is preserved until the degradation temperature is reached, which significantly enhances the material's dimensional stability as well as its resistance to creep and solvent stress cracking.[3,5,6] Nevertheless, as consequence of the

resulting decrease in viscosity according to the Arrhenius relation, associative CANs offer repairability and recyclability comparable to thermoplastic materials.[7]

In associative CANs, numerous exchange mechanisms have been extensively studied and frequently applied. These mechanisms include transesterification,[8] transcarbamoylation,[9] thiol-thioester exchange,[10] and siloxane exchange,[11] which can be conveniently catalyzed using conventional organic bases. By introducing a simple organic base, the dynamic exchange of covalent bonds is permanently catalyzed and can only be regulated as a function of temperature (**Figure 1a**). Thus, a precisely defined and moreover spatially resolved onset of topological rearrangements is not possible.[5,12,13] To address this substantial drawback, photolatent and thermolatent base generators have been developed and introduced in CANs. Through a controlled (spatially resolved) light or temperature mediated release of the active catalyst an optimized creep resistance of the polymer network's initial state, has been achieved (**Figure 1b**). However, as the activation process is irreversible, the original mechanical properties (e.g., low creep) of the material cannot be restored after one-time activation for reshaping, welding, or recycling.[14,15]

Recently, different attempts using reversibly (thermo-)switchable catalysts have been made.[16,17] Sardon and co-workers for example synthesized a quaternary ammonium salt capable of undergoing reversible thermal dissociation under the release of a strong guanidine base. Compared to the permanently free catalyst, rates for covalent bond exchange were significantly reduced below 100 °C, while with increasing temperature almost comparable rates were achieved. The concept nevertheless is still based on a thermal dissociation equilibrium and did not enable an ON/OFF-like behavior, i.e., different material properties at the same temperature. Accordingly, a spatially resolved catalyst activation, important for precise reshaping or welding applications, was not feasible.[17]

Herein, we present an advanced approach for the reversible activation/deactivation of a photoswitchable nitrogen superbase within a thiol-ene photopolymer (**Figure 1c**). The substantial temperature-decoupled difference in pK_a between the isomeric states enables spatially resolved reversible control over the dynamic, associative exchange between thioester links and thiol groups. This is demonstrated by stress relaxation, reshaping, micro-imprint and tensile testing experiments. To understand the catalytic process in more detail, we additionally performed quantum chemical calculations using density functional theory (DFT).

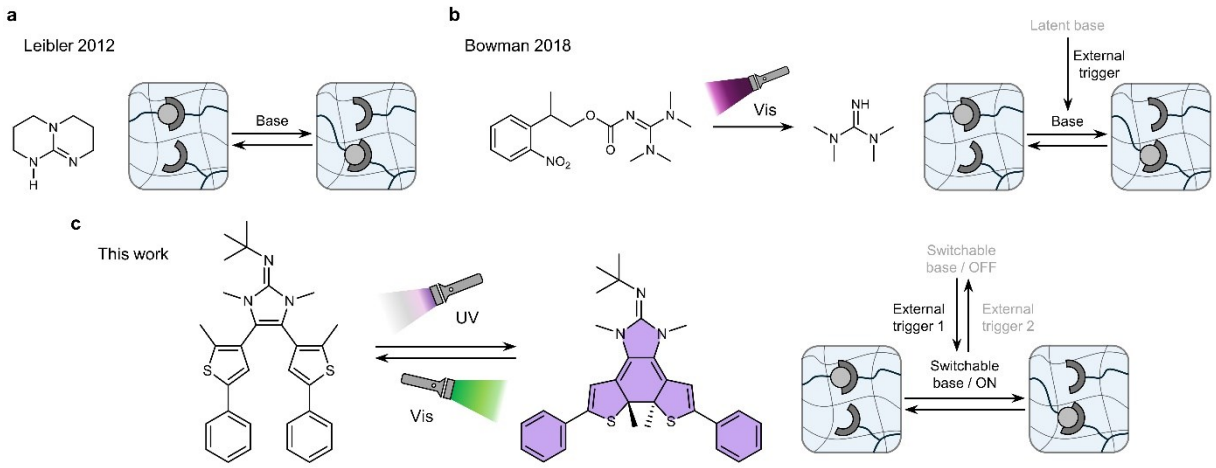

Figure 1. Schematic illustration of the conceptional evolution of base-catalyzed CANs. a) Conventional CANs in which bond exchange is catalyzed by a simple organic base. b) First stage of evolution using latent base catalysts for an irreversible on-demand activation of the active catalytic species. c) The herein presented second stage of evolution using a switchable base catalyst for a reversible activation of bond exchange.

2. Results and Discussion

2.1. Design of a Photoswitchable CAN

As a photoswitchable base catalyst (PSBC), an *N*-heterocyclic imine, consisting of a photochromic dithienylethene derivative equipped with a guanidine unit, was applied. Photoreversible electrocyclic isomerization proceeds without sterically demanding rearrangements in the order of seconds upon successive irradiation with UV and visible light. In combination with the accompanied difference in pK_a of 8.7 between the ring-opened (25.7) and ring-closed (17.0) state, and its thermal stability, the *N*-heterocyclic imine possesses ideal properties to be applied as PSBC in CANs. A ^{1}H NMR spectrum of the final product, synthesized in six steps according to the literature,[18] are shown in **Figure S1** (Supporting Information).

Pioneered and thoroughly studied by Bowman and co-workers, the base-catalyzed associative exchange between thioester links and thiol groups was applied for dynamic rearrangement of the network topology, as it occurs rapidly even at low catalyst concentrations.[10,14,19] Thioester links were brought into the system via a diallyl ether monomer (TEDA) synthesized according to the literature.[14] Its structure was confirmed by ^{1}H NMR spectroscopy (**Figure S2**, Supporting Information). As a commercially available tetra-functional thiol crosslinker, pentaerythritol tetrakis(3-mercaptopropionate) (PETMP) was used in a 1:1 molar ratio to TEDA,

which corresponds to a 100 % excess of thiol groups. All samples were prepared with a PSBC content of 0.7 mol%. In addition, 0.7 mol% ethyl mesitylcarbonyl(phenyl)phosphinate (TPO-L) were added to induce radical thiol-ene photopolymerization by 405 nm LED light, which enabled quantitative yields in high rates under mild reaction conditions. FTIR spectra recorded prior to and after polymerization (**Figure S3**, Supporting Information) show a complete alkene (3084 cm^{-1}) conversion whilst only half of the thiol groups (2571 cm^{-1}) are consumed. Thioester links, visible at 1689 cm^{-1}, remain unaffected. The presence of free, unreacted thiol groups after polymerization is essential to enable network rearrangements through the base-catalyzed dynamic exchange with thioester links. The resulting polymer structure exhibited a glass transition temperature of -30 °C, based on differential scanning calorimetry (DSC, **Figure S4**, Supporting Information), and superior thermal stability. In thermogravimetric analysis (TGA), the total mass loss remained below 1 % up to a temperature of 280 °C (**Figure S5**, Supporting Information).

To avoid interfering absorption with the radical photoinitiator at 405 nm during polymerization, the PSBC was incorporated in the polymer in its transparent ring-opened state. Photoswitching to the dark blue colored ring-closed state was performed using 313 nm LED light, whereas visible broadband LED light was used to reobtain the transparent ring-opened state. **Figure S6** (Supporting Information) summarizes the emission spectra and intensity values of all irradiation sources used, and **Figure 2a** provides a schematic overview of the mechanistic concept pursued along with the chemical structures of all formulation components used.

Dissolved in the photopolymer, the PSBC's ring-closed state appeared dark blue in color, compared to its purple appearance in acetonitrile, which can be explained by protonation through the present thiol groups. In support of this statement, UV-Vis measurements in acetonitrile showed a shift in the absorption maximum of the ring-closed isomer from 567 nm to 615 nm upon protonation with diluted $HClO_4$, while the absorption maximum of the ring-opened isomer at about 273 nm remained almost unaffected (**Figure 2b**).

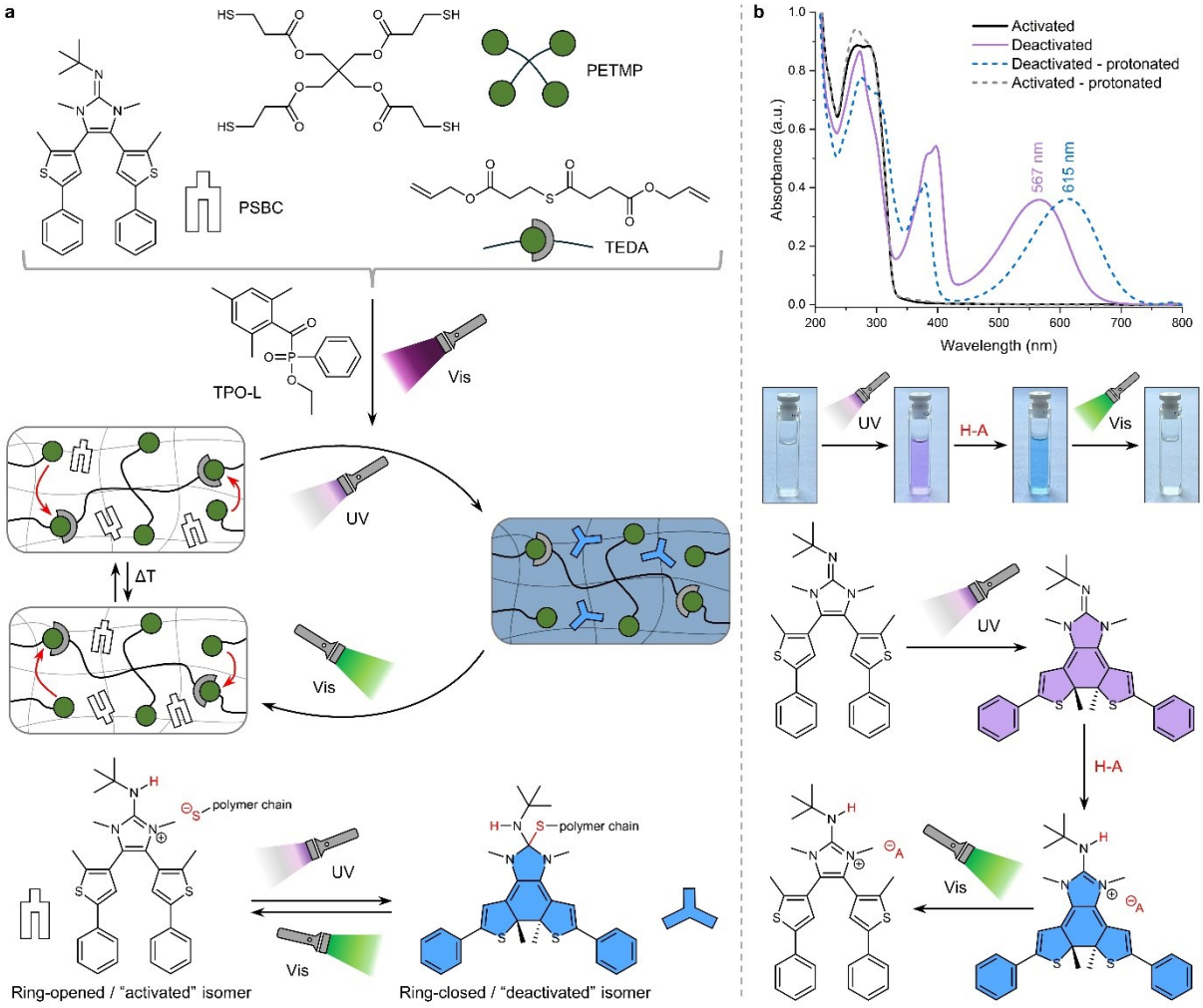

Figure 2. Conceptional design of a photoswitchable CAN. a) Chemical structures and schematic symbols of the formulation components used together with a schematic representation of the light-mediated switching of the PSBC within the resulting thiol-ene photopolymer, enabling control over the base-catalyzed dynamic exchange between thioester links and thiol groups. b) Absorption behavior and chemical structures of the PSBC in its activated (ring-opened), deactivated (ring-closed), deactivated protonated, and activated protonated state in acetonitrile (3×10^{-5} mol L^{-1}), H-A = $HClO_4$.

Quantum chemical DFT calculations were performed to gain a better understanding of the structural and catalytic properties of the PSBC used (see the Supporting Information for details). Methyl-3-mercaptopropionate (MMP) was considered to mimic the thiol groups in the polymer matrix, as it corresponds to one side chain of the PETMP molecule. Exothermic deprotonation of MMP by the PSBC is predicted for both the ring-opened catalyst (-86.0 kJ mol^{-1}) and the ring-closed catalyst (-54.8 kJ mol^{-1}), which is consistent with the experimental observations. Minimum energies of all calculated individuals are listed in **Table S1** (Supporting Information). The minimum structures of the resulting PSBC/MMP adducts are shown in **Figure 3**. In the ring-closed adduct, a covalent C-S bond with a length of 1.96 Å is formed, resulting in an overall neutral species with a tetrahedrally coordinated carbon atom. In contrast, the guanidine unit in the ring-opened form remains planar, resulting in an ionic adduct with a C-S distance of 3.67 Å. Accordingly, with respect to the transesterifications, the weakly bound thiolate group of the ionic adduct is expected to be a highly active nucleophile, while the neutral ring-closed adduct represents a deactivated state, as dissociation into solvated ions require approx. 100.0 kJ mol^{-1} in energy.

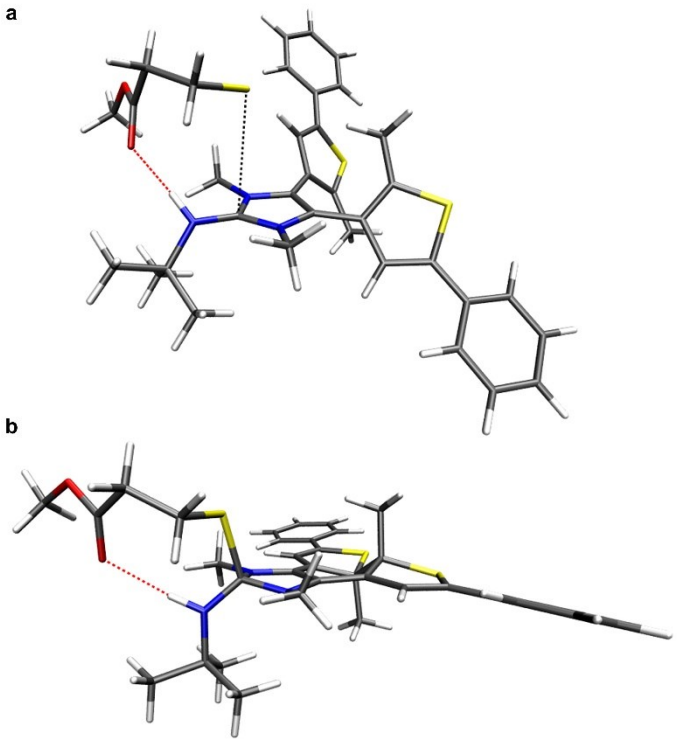

Figure 3. a, b) Calculated minimum structures for the ring-opened (a) and ring-closed (b) PSBC/MMP adduct. Obtained at B3LYP/6-311++G(d,p)/SMD level of theory, red dashed lines indicate hydrogen bonds, while the C-S contact of 3.67 Å in the ring-opened form is indicated by a black dashed line. (colors: C gray, H white, O red, N blue, S yellow).

2.2. Reversible Switching of the PSBC

Analyzed by the absorption behavior of a 50 µm thick polymer film, only 58 mJ cm^{-2} of UV light, corresponding to an irradiation time of 22 s, were needed for quantitative switching to the less basic ("deactivated") ring-closed isomer (**Figure 4a**). On the other hand, a visible light exposure dose of 6817 mJ cm^{-2}, corresponding to an irradiation time of 160 s, had to be applied for reobtaining the more basic ("activated") ring-opened isomer (**Figure 4b**).

To analyze the fatigue behavior of photoreversible switching, ten full cycles were monitored by UV-Vis analysis (**Figure 4c**). Overall, an excellent fatigue resistance was observed, although minor by-product formation was indicated by an increasing absorption peak at 581 nm in the course of the experiment. Concurrently, the absorption peak at 624 nm, assigned to the deactivated state of the PSBC, was marginally diminishing. As reported in several studies, the ring-closed isomers of different diarylethene derivatives are prone to side reactions such as photochemical elimination, or oxidation.[20,21] Upon excitation with UV light, however, the formation of an annulated ring system by a formal 1,2-dyotropic rearrangement is predominantly described. In accordance with our observations, these irreversibly formed by-products resemble the length of π-conjugation of the corresponding ring-closed isomers and show therefore a similar, but slightly hypsochromically shifted, absorption behavior.[20,22,23]

Since the PSBC was present dissolved in a (solid) covalently-crosslinked photopolymer, spatially resolved photoswitching, i.e., isomerization, was facilitated. The significant difference in the absorption behavior between the activated and deactivated state additionally enabled reversible, light-controlled drawing of different icons as shown in **Figure 4d**.

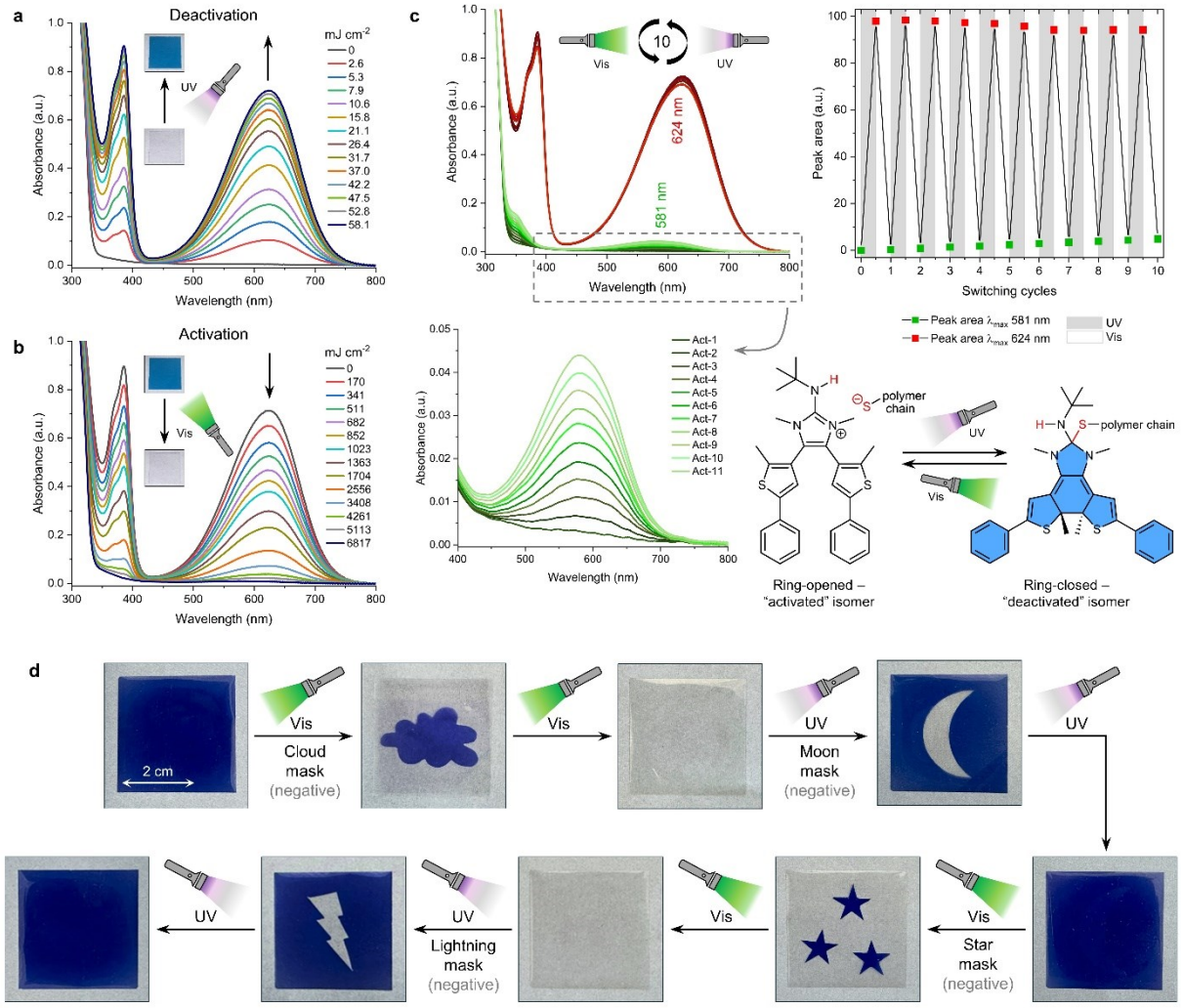

Figure 4. UV-Vis absorption behavior and switching kinetics of a 50 µm thick photopolymer film containing 0.7 mol% PSBC in its protonated state. a) Absorption behavior in the course of deactivation using UV light. b) Absorption behavior in the course of activation using visible light. c) Fatigue resistance of the PSBC in its protonated state (illustrated in chemical structures) followed upon successive irradiation with UV and visible light over ten full switching cycles. d) Locally controlled drawing, erasing, and redrawing of different icons mediated by UV and visible light.

2.3. Mechanical Network Properties

Base-catalyzed dynamic bond exchange was examined by stress relaxation experiments at 70 °C using a universal extensional fixture in combination with a convection temperature device (**Figure S7**, Supporting Information). First, six consecutive measurements with reversible switching between the activated and deactivated state of the PSBC were performed (**Figure 5a**). Starting from the activated, i.e., ring-opened, state, the 50 µm thick specimen showed an immediate decrease of the normalized relaxation modulus (G/G_0) to 10 % within 300 s (Act). Following irradiation with UV light to generate the deactivated, i.e., ring-closed, state, a subsequent measurement was carried out with the same specimen (Deact). Due to the considerably lowered basicity, topological rearrangements of the covalently cross-linked network, by the base-catalyzed exchange between thioester links and thiol groups, proceeded significantly slower. Within the same measurement time of 300 s, (G/G_0) decreased only to 71 %. Prior the third consecutive measurement (Act-2), the specimen was exposed to visible light for regeneration of the PSBC's activated state. Owing to the re-increased basicity and rate of dynamic bond exchange, a stress relaxation rate comparable to the first measurement in the activated state (Act), decrease of (G/G_0) to 11% within 300 s, was successfully achieved.

During the fourth consecutive measurement, i.e., second measurement conducted in the deactivated state (Deact-2), (G/G_0) decreased to 67 %. In comparison with the first measurement (Deact), the slightly increased stress relaxation rate can be attributed to the irreversible formation of small quantities of by-product, as detected by UV-Vis experiments (Figure 4c). Measurements Act-3 and Deact-3 exhibited a continuation of this trend and indicated a basicity of the by-product between that of the activated and deactivated isomer.

In addition, three consecutive measurements in the activated as well as in the deactivated state were performed. While all the relaxation curves obtained in the activated state are almost congruent (**Figure S8a**, Supporting Information), the measurements in the deactivated state showed a slightly increasing stress relaxation rate (**Figure S8b**, Supporting Information) indicating a minor temperature-induced recovery of the activated state, i.e., ring-opened isomer.

For concurrent visualization of the different stress relaxation properties of the activated and deactivated state, two 1.39 mm wide lines of a deactivated test specimen were irradiated with visible light. These transparent, activated areas were separated by a 1.62 mm wide line still in in the deactivated state (**Figure 5b**). Same as for all the other stress relaxation experiments, the specimen was elongated at 70 °C for 300 s. After completion of the experiment, the deactivated center line's width changed marginally to 1.64 mm because rearrangements of the covalently cross-linked network structure were limited in the presence of the less basic ring-closed isomer.

However, both lines containing the activated, i.e., ring-opened, PSBC increased their width considerably, owing to the dynamic exchange between thioester links and thiol groups, and equaled the 1.64 mm of the center line. Moreover, a distinct constriction of the specimen's outline was observed due to the strong relaxation concentrated in these areas.

To confirm that the topological network reorganization process is based on an associative bond-forming, bond-breaking reaction sequence, stress relaxation measurements were conducted on an activated sample between 70 and 110 °C (**Figure 5c**). Toward higher temperatures, the accelerated dynamic exchange between thioester links and thiol groups led to lower characteristic relaxation times (τ). Based on the assumption of a generic exponential behavior, i.e., $(G_{(t)}/G_0) = exp(-t/\tau)$, values for τ were obtained at the point at which $(G_{(t)}/G_0)$ decreased to $(1/e)$. Plotted against the reciprocal of the temperature, a linear trend according to the Arrhenius relation was observed (**Figure 5d**). Therefore, the temperature independence of the global number of cross-links and the related associative nature of the mechanism for dynamic bond exchange were substantiated.[12,13,24]

Apart from stress relaxation experiments, we utilized the ability to deliberately induce a base-catalyzed exchange of covalent bonds for a controlled training of the polymer's mechanical properties (**Figure 5e**). By stimulating the dynamic exchange between thioester links and thiol groups in the presence of an excess of a free low-molecular weight thiol in the surrounding gas phase, an incorporation of thiols into the network structure was achieved. This led to a reduction in the number of cross-links. Activated samples treated with thiol at 70 °C for 20 min exhibited an about 55 % lower Young's modulus of 7.0 ± 0.6 kPa, compared to activated non-treated samples (15.5 ± 0.2 kPa). For in parallel treated deactivated samples, on the other hand, a decrease in the Young's modulus of only about 9 % to 14.1 ± 0.8 kPa was determined. Due to the significantly lower activity of the ring-closed isomer of the PSBC in the dynamic exchange between thioester links and thiol groups, the number of thiol molecules incorporated from the surrounding gas phase and the resulting decrease in cross-link density of the network structure were considerably limited. Consequently, we successfully created a photoswitchable associative CAN suitable for undergoing a light-controlled softening process.

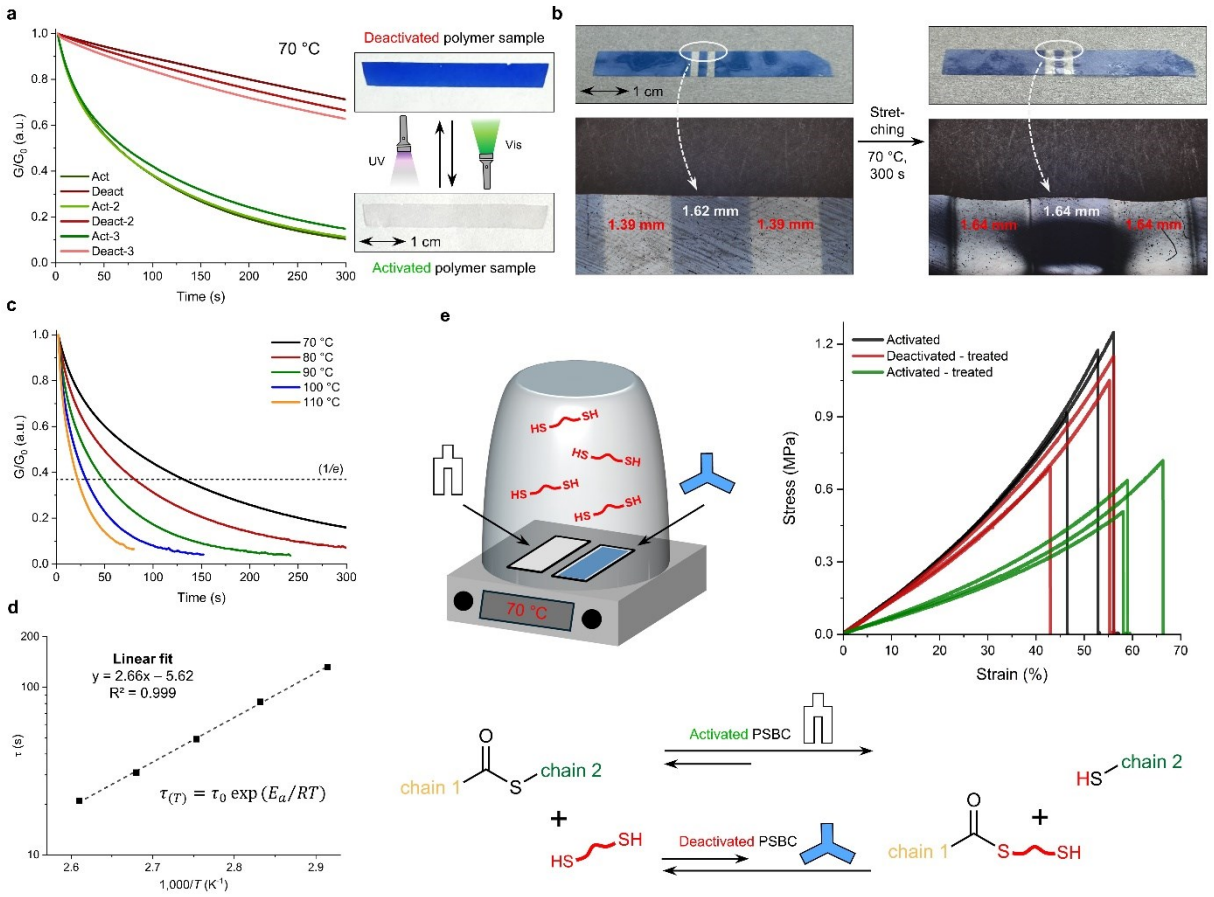

Figure 5. Mechanical properties of the polymer structure. a) Normalized stress relaxation data obtained from the same specimen at 70 °C upon successive reversible switching between the activated and deactivated state of the PSBC. b) Visualization of the stress relaxation behavior of activated and deactivated parts of a test specimen by stretching at 70 °C for 300 s. c) Normalized stress relaxation data obtained from an activated test specimen in a temperature range of 70 to 110 °C. d) Arrhenius plot of the characteristic relaxation times (τ) determined at a decrease of the respective normalized relaxation modulus (G/G_0) to $1/e$. Insets show the corresponding Arrhenius relation and parameters used for linear fitting. E_a is the activation energy, R the universal gas constant, and R^2 the coefficient of determination. e) Tensile properties of the polymer structure after controlled softening induced by the incorporation of a low molecular weight thiol from the surrounding gas phase at 70 °C.

2.4. Reshaping and Micro-Imprinting

To demonstrate the spatially resolved photoreversible activation of dynamic bond exchange, confirmed by different stress relaxation and tensile testing experiments, in an application-based manner, we performed a multi-step reshaping experiment (**Figure 6a**). In the first step, only the right half of the fully deactivated rectangular test specimen was irradiated with visible light to locally generate the activated, i.e., ring-opened, state of the PSBC. Subsequently, the specimen was pressed into a corrugated mold, and the whole setup was stored at 70 °C for 7 min. Throughout this period, the network topology of the right half was reorganized against the applied force, or rather according to the predefined corrugated shape, by the base-catalyzed exchange between thioester links and thiol groups. Hence, a new shape was obtained that remained in position even after the mold was removed. The test specimen's left half, however, immediately returned to the entropically more favorable straight position as the cross-linked network structure defined during polymerization was only altered to a limited extend. After the activated state of the PSBC was generated in the entire test specimen using visible light, the thermal molding process was repeated to create a uniform corrugated shape. The following step was to expose only the right half of the test specimen to UV light to restore the deactivated state, i.e., the ring-closed isomer, of the PSBC in this area. Afterwards, a flat mold was used for fixation and storage at 70 °C for 7 min to bring only the still activated, transparent left half of the test specimen back in its initial flat shape by the spatially resolved dynamic exchange of covalent bonds. In the final step, the original uniformly flat shape was restored after exposing the entire test specimen to visible light.

We further exploited the successfully demonstrated material's ability for the spatially resolved reversible activation of dynamic bond exchange for light-controlled micro-imprinting (**Figure 6b**). First, the upper half of the fully activated square test specimen (7 x 7 mm), functioning as the substrate, was exposed to UV light to locally generate the deactivated, i.e., ring-closed, state of the PSBC. Afterwards, the substrate was clamped onto an imprinting mold and stored at 70 °C for 7 min to create about 50 µm wide lines in vertical direction. Since the base-catalyzed exchange between thioester links and thiol groups was substantially suppressed in the blue colored upper half, lines were imprinted only in the lower half containing the PSBC in its activated state. For the second step, the deactivated state of the PSBC was generated in the left half of the substrate, and imprinting was repeated at an angle of 90 °. Following the same principle, lines became visible only in the transparent activated part of the substrate as reorganization of the network topology according to the shape of the imprinting mold proceeded significantly faster in the presence of the more basic ring-opened isomer of the PSBC.

Consequently, four separate sections were created: (1) deactivated in both imprinting steps, no lines; (2) activated in the second imprinting step, lines in horizontal direction; (3) activated in the first imprinting step, lines in vertical direction; (4) activated in both imprinting steps, lines in both directions (checked pattern). Owing to the light-controlled spatially resolved activation of dynamic bond exchange, we were able to develop a novel imprinting concept suitable for producing versatile intersecting structures under the use of just a single imprinting mold. Moreover, it enables the erasure of imprints by compressing the substrate in its activated state between flat PTFE-coated surfaces at 90 °C for 20 min (**Figure S9**, Supporting Information).

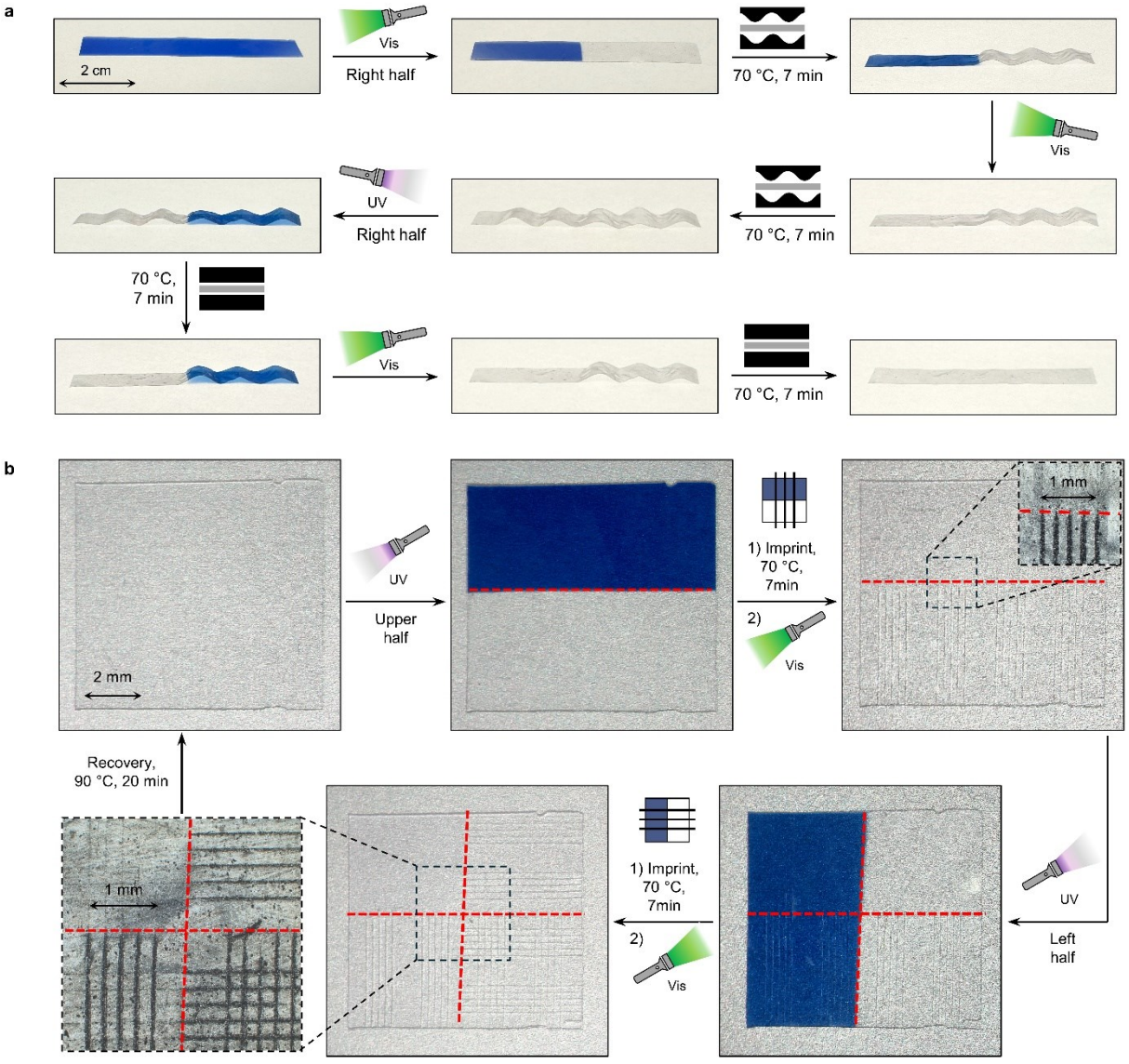

Figure 6. a, b) Multi-step reshaping (a) and micro-imprinting (b) experiments based on the spatially resolved, reversible activation of the PSBC within the polymer matrix upon successive exposure to UV and visible light.

Although, restrictions in sample geometry and layer thickness apply, mainly by the penetration depth of the UV light used for activation, targeted modification of the PSBC offers a potential remedy. As described by Hecht and co-workers, for example, a bathochromic shift of the absorption maximum of diarylethenes can be induced by the introduction of an intramolecular triplet sensitizer, which can additionally prevent the irreversible formation of an annulated ring system as a by-product.[22]

3. Conclusion

As evidenced by different UV-Vis and stress relaxation experiments, the application of a photoswitchable nitrogen superbase in a dynamic polymer system enabled spatially resolved and reversible network reorganization by exchanging thioester links and thiol groups. Quantum chemical calculations suggested that deactivation of the ring-closed PSBC resulted from the formation of a covalent C-S bond between the thiolate and the protonated guanidine base. In contrast, the thiolate group remained unbound in the ring-opened state of the PSBC and thus highly active for transesterifications. Light-controlled softening was able to be induced by the incorporation of a low molecular weight thiol, and reshaping as well as micro-imprinting experiments revealed prospective application areas.

Overall, the herein presented system significantly improved the conceptional sophistication of CANs by providing a locally controlled, reversible, and temperature-decoupled regulation of dynamic bond exchange. It offers universal applicability in CANs relying on a base-catalyzed exchange mechanism, and additional application in 3D printing or recycling are conceivable.

Supporting Information

Supporting Information is available.

Acknowledgements

The research was carried out within the COMET-Module project ”Repairtecture” (project-no.: 904927) at the Polymer Competence Center Leoben GmbH (PCCL, Austria) within the framework of the COMET-program of the Federal Ministry for Climate Action, Environment, Energy, Mobility, Innovation and Technology and the Federal Ministry of Labour and Economy. Funding was provided by the Austrian Government and the State Governments of Styria and Upper Austria.

Thanks are due to the Universität Innsbruck for a PhD fellowship (A.S.).

Conflict of Interest

The authors declare no conflict of interest.

Author Contributions

A.S. and A.D. contributed equally to this work. S.S., F.G., and F.D. performed project administration, acquired funding and supervised the work. S.S., E.R., and D.R. conceptualized the experiments with the exception of quantum chemical calculations. A.S. and A.D. synthesized and characterized (NMR) the photoswitchable base catalyst. S.P. synthesized and characterized (NMR) the thioester-containing diallyl ether monomer. M.W. and S.H. supervised stress relaxation experiments. F.D. and T.S.H. conceptualized quantum chemical calculations. T.S.H. performed quantum chemical calculations. D.R. performed all other experimental work including data analysis and wrote the original draft. S.S., T.S.H., F.D., and A.D. edited the manuscript. All authors reviewed the article.

References

[1] a) D. Ratna, *Recent Advances and Applications of Thermoset Resins*, Elsevier, Amsterdam, Netherlands **2022**; b) J.-P. Pascault, R. J. J. Williams in *Handbook of Polymer Synthesis, Characterization, and Processing* (Eds.: E. Saldíva-Guerra, E. Vivaldo-Lima), Wiley, Hoboken, NJ, USA **2013**; c) E. Morici, N. T. Dintcheva, *Polymers* **2022**, *14*, 4153.

[2] W. Alabiso, S. Schlögl, *Polymers* **2020**, *12*, 1660.

[3] J. M. Winne, L. Leibler, F. E. Du Prez, *Polym. Chem.* **2019**, *10*, 6091.

[4] a) M. A. Shirai, J. Zanela, M. H. Kunita, G. M. Pereira, A. F. Rubira, C. M. O. Müller, M. V. E. Grossmann, F. Yamashita, *Adv. Polym. Technol.* **2018**, *37*, 332; b) J. Momanyi, M. Herzog, P. Muchiri, *Recycling* **2019**, *4*, 33.

[5] F. Van Lijsebetten, T. Debsharma, J. M. Winne, F. E. Du Prez, *Angew. Chem. Int. Ed.* **2022**, *61*, e202210405.

[6] M. Podgórski, B. D. Fairbanks, B. E. Kirkpatrick, M. McBride, A. Martinez, A. Dobson, N. J. Bongiardina, C. N. Bowman, *Adv. Mater.* **2020**, *32*, 1906876.

[7] a) F. Meng, M. O. Saed, E. M. Terentjev, *Nat. Commun.* **2022**, *13*, 5753; b) K. W. J. Ng, J. S. K. Lim, N. Gupta, B. X. Dong, C.-P. Hu, J. Hu, X. M. Hu, *Commun. Chem.* **2023**, *6*, 158; c) H. Zhang, J. Cui, G. Hu, B. Zhang, *Int. J. of Smart Nano Mater.* **2022**, *13*, 367.

[8] T. Liu, B. Zhao, J. Zhang, *Polymer* **2020**, *194*, 122392.

[9] X. Chen, L. Li, K. Jin, J. M. Torkelson, *Polym. Chem.* **2017**, *8*, 6349.

[10] A. S. Kuenstler, C. N. Bowman, *ACS Macro Lett.* **2023**, *12*, 133.

[11] T. Debsharma, V. Amfilochiou, A. A. Wróblewska, I. de Baere, W. van Paepegem, F. E. Du Prez, *J. Am. Chem. Soc.* **2022**, *144*, 12280.

[12] M. Guerre, C. Taplan, J. M. Winne, F. E. Du Prez, *Chem. Sci.* **2020**, *11*, 4855.

[13] M. Capelot, M. M. Unterlass, F. Tournilhac, L. Leibler, *ACS Macro Lett.* **2012**, *1*, 789.

[14] B. T. Worrell, M. K. McBride, G. B. Lyon, L. M. Cox, C. Wang, S. Mavila, C.-H. Lim, H. M. Coley, C. B. Musgrave, Y. Ding, C. N. Bowman, *Nat. Commun.* **2018**, *9*, 2804.

[15] a) D. Reisinger, M. U. Kriehuber, M. Bender, D. Bautista-Anguís, B. Rieger, S. Schlögl, *Adv. Mater.* **2023**, *35*, 2300830; b) D. Reisinger, S. Kaiser, E. Rossegger, W. Alabiso, B. Rieger, S. Schlögl, *Angew. Chem. Int. Ed.* **2021**, *60*, 14302; c) D. Reisinger, A. Hellmayr, M. Paris, M. Haas, T. Griesser, S. Schlögl, *Polym. Chem.* **2023**, *14*, 3082; d) D. Reisinger, K. Dietliker, M. Sangermano, S. Schlögl, *Polym. Chem.* **2022**, *13*, 1169.

[16] a) F. Van Lijsebetten, S. Maes, J. M. Winne, F. E. Du Prez, *Chem. Sci.* **2024** *15*, 7061; b) G. Vozzolo, F. Elizalde, D. Mantione, R. Aguirresarobe, M. Ximenis, H. Sardon, *Polymer* **2024**, *302*, 127051.

[17] G. Vozzolo, M. Ximenis, D. Mantione, M. Fernández, H. Sardon, *ACS Macro Lett.* **2023**, *12*, 1536.

[18] L. F. B. Wilm, M. Das, D. Janssen-Müller, C. Mück-Lichtenfeld, F. Glorius, F. Dielmann, *Angew. Chem. Int. Ed.* **2022**, *61*, e202112344.

[19] a) B. T. Worrell, S. Mavila, C. Wang, T. M. Kontour, C.-H. Lim, M. K. McBride, C. B. Musgrave, R. Shoemaker, C. N. Bowman, *Polym. Chem.* **2018**, *9*, 4523; b) C. Wang, S. Mavila, B. T. Worrell, W. Xi, T. M. Goldman, C. N. Bowman, *ACS Macro Lett.* **2018**, *7*, 1312; c) J. J. Hernandez, S. P. Keyser, A. L. Dobson, A. S. Kuenstler, C. N. Bowman, *Macromolecules* **2024**, *57*, 1426.

[20] M. Herder, B. M. Schmidt, L. Grubert, M. Pätzel, J. Schwarz, S. Hecht, *J. Am. Chem. Soc.* **2015**, *137*, 2738.

[21] a) K. Higashiguchi, K. Matsuda, T. Yamada, T. Kawai, M. Irie, *Chem. Lett.* **2000**, *29*, 1358; b) H. Liu, Y. Chen, *New J. Chem.* **2012**, *36*, 2223; c) H. Shoji, S. Kobatake, *Chem. Commun.* **2013**, *49*, 2362.

[22] S. Fredrich, R. Göstl, M. Herder, L. Grubert, S. Hecht, *Angew. Chem. Int. Ed.* **2016**, *55*, 1208.

[23] S. Qiu, A. T. Frawley, K. G. Leslie, H. L. Anderson, *Chem. Sci.* **2023**, *14*, 9123.

[24] a) W. Alabiso, B. Sölle, D. Reisinger, G. La Guedes de Cruz, M. Schmallegger, T. Griesser, E. Rossegger, S. Schlögl, *Angew. Chem. Int. Ed.* **2023**, *62*, e202311341; b) D. Montarnal, M. Capelot, F. Tournilhac, L. Leibler, *Science* **2011**, *334*, 965.